WaveComBE

mmWave Communications in the Built Environments

WaveComBE_D1.1

Massive MIMO antenna numerical model

Version v1.0 Date: 2019/05/08

Document properties:

WaveComBE_D1.1 Massive MIMO antenna numerical model.

Grant Number:	766231
Document Number:	D1.1
Document Title:	Massive MIMO antenna numerical model
Partners involved:	University of Twente, Gapwaves
Authors:	Andrés Alayón Glazunov , Wai Yan Yong, Alireza Bagheri, Carlo Bencivenni, Thomas Emanuelson
Contractual Date of Delivery:	2019/03/08
Dissemination level:	PU[1]
Version:	1.0
File Name:	WaveComBE D1.1_v1.0

[1] CO = Confidential, only members of the consortium (including the Commission Services)

[2] PU = Public

Table of contents

Executive Summary

The development of advanced antenna technologies and designs is at the core of 5G communications systems. In this report, we present numerical designs based on two approaches for antenna design at the mmWave (millimeter wave) frequencies.

In the first approach we propose a high gain microstrip grid array antenna (GAA) with enhanced bandwidth performance for fixed beam mmWave point-to-point applications. Two bandwidth enhancement techniques have been considered, the first is to use rhombus shaped radiating elements on the short radiating sides of the conventional GAA, and the second technique is to replace the conventional short radiating sides with the staircase elements. Employing the rhombus elements on the short sides of the GAA structure provides additional capacitive reactance which allows to cancel out the inductive reactance in the conventional GAA leading to bandwidth enhancement. The resulting -10 dB impedance bandwidth is 16%, from 27.5 GHz to 32 GHz with the maximum achieved gain of 14.8 dBi. In the second technique, replacing the short sides of the GAA by a staircase provides a longer current path which leads to the bandwidth enhancement. The second solution, as compared to the first one, provides more flexibility in the bandwidth optimization. Indeed, the second proposed technique provides a -10 dB impedance bandwidth of 21% ranging from 23.5 GHz to 29.5 GHz and a maximum gain of 12.5 dBi. The slight reduction in gain performance is mainly attributed by the removal of some radiating elements to ensure low side lobes level on the radiation pattern.

In the second design approach, which is more promising, we propose the design of a mmWave multibeam antenna array for base station applications based on the gap waveguide (Gapwaves waveguide) technology. The proposed antenna operates from 26.5 GHz up to 29.5 GHz, i.e., an operating bandwidth of 10.7% with maximum gain of 23.7 dBi. Numerical simulations show that the proposed antenna provides a scanning angle of ±45° over the azimuth plane with embedded matching and isolation better than -16 dB, while the simulated active matching is better than -10 dB at all scan angles. Based on the simulation results, we conclude that the proposed array antenna is a potential candidate as a 5G Massive MIMO indoor base station antenna.

List of figures

List of tables

List of Acronyms and Abbreviations

GAA	Grid Array Antenna
MIMO	multiple-input multiple-output
FSS	Frequency Selective Surface
LTCC	Low Temperature Co-fired Ceramic
FCC	Federal Communications Commission
AT	Amplitude-Tapering
SLL	Side-Lobes Level
CEPT	European Conference of Postal and Telecommunications Administration
mmWave	millimeter wave
PCB	printed circuit board
PEC	perfect electric conductor
PMC	perfect magnetic conductor

1. Introduction

The proliferation of new wireless applications such as the Internet of things (IoTs), machine-to-machine (M2M) communications, E-health, E-business and E-learning is leading to a greater demand of much higher data rate communication services to multiple users or machines [1]. In order for the 5G wireless communication networks be capable to support data rates of the order of 1 - 10 Gb/s , the millimetre wave (mmWave) bands have been identified to accommodate the new systems in addition to the sub-6 GHz bands [1]–[3]. However, as compared to the lower frequency bands, the propagation path loss at the mmWaves is significantly higher [3]. To compensate for it, antennas that will be employed are expected to come with high gain performance [2]. Therefore, advanced multiple antenna techniques have been proposed for 5G such as massive multiple-input multiple-output (MIMO) and beamforming techniques [4]–[6]. These techniques can increase the gain of the antennas towards the user while at the same time provide better interference suppression capabilities. Given the huge number of antenna elements that are needed, it is crucial to develop mmWave array antennas that are low cost, low complexity, with large wideband, good integration capability and low profile.

The existing mmWave antennas proposed for satellite communication and radar systems such as the reflectarray antenna [7], [8] and waveguide-based phased array antenna [9], [10] have been proved to work well. Nevertheless, these antenna systems are too large and too expensive to be employed for commercial terrestrial mmWave communication systems that require a huge number of small cell base stations. In addition, the waveguide-based phased array antennas are expensive to manufacture as they require high precision manufacturing and close electrical contact between layers. To lower the manufacturing cost and antenna size, the coplanar waveguide (CPW) and the substrate integrated waveguide (SIW) technologies [11] have been proposed for integration of antennas with passive microwave devices in multi-layer stacking structures. However, with the presence of the dielectric substrate, these proposed antenna systems do not achieve high gain performance as the transmission lines built up from these two technologies also suffer from high dielectric and ohmic losses and radiation leakage, especially at the high mmWave frequencies. In [12] , antenna design based on frequency selective surface (FSS) is proposed to improve the antenna gain. However, when the FSSs are cascaded, the antenna bandwidth decreases. Recently, a grid array antenna has been proposed to realize a wideband, high gain antenna for mmWave applications using multilayer low temperature co-fired ceramic (LTCC) substrate [13]. Although the LTCC technology manages to provide a good performance, the fabrication process is complicated and incur in high fabrication costs. Therefore, the proposed solutions become less practical for 5G base stations since a huge number of base stations are expected to be built and a large number of antennas will be employed. A practical solution offering low profile features can be designed using the conventional printed circuit board (PCB) technology [14]. However, conventional microstrip antenna employed in previous generations of communication system is no longer feasible due to the high materials losses. In addition, the surface waves and higher order modes can also be generated especially in the presence of discontinuities, bends, open ends and steps that commonly appear in the design of feeding network of the antennas.

In Section 2 of this paper, a broadband microstrip grid array antenna (GAA) is presented that is designed to be directly fed from a 50 Ω coaxial line without an impedance transformer. The wideband GAA is realized by loading a rhombus shaped element into the short radiating sides of the GAA. The broadband mmWave GAA with low complexity and compact size is proposed for 5G communication system without the need of using multilayer stacking or complicated LTCC technology.

In Section 3 of this paper, a solution is proposed to devise a high gain mmWave antenna for Massive MIMO antenna systems that is able to integrate numerous of passive components. We use the recently proposed gap waveguide technology commercialized by Gapwaves AB, which is one of the members of the WAVECOMBE project consortium. The proposed multibeam scanning antenna array solution has been devised to work within the 26.5-29.5 GHz band as a 5G Massive MIMO base station.

2. Fixed-beam high-gain microstrip grid array antenna (GAA) with enhanced bandwidth performance

The conventional GAA is composed of rectangular loops of conductors above a ground plane with a single or multiple feed points [15], [16] . The conventional GAA is designed to have a long side grid length of L_g and short side grid length of $\lambda_g/2$, where λ_g is the guided wavelength [15]. The long sides of the grid have an out of phase instantaneous current distribution and the short sides of the grid have in-phase instantaneous current distribution. Although the conventional GAA has been proven to have a good radiation performance, the impedance bandwidth performance is still insufficient to cover the entire proposed 5G frequency band as recommended by the Federal Communications Commission (FCC). This is because the microstrip straight line radiating elements have a narrow bandwidth [15].

Two techniques are proposed here to enhance the conventional GAA operating at the mmWave band. The first technique is to load the rhombus shaped radiating element on the short sides of the conventional GAA and the second technique is to replace the conventional slot on the short sides of the GAA with the staircase radiating elements. Both of the proposed GAAs are designed on the 0.787-mm-thick Rogers RT 5880 substrate with dielectric constant of 2.2 and loss tangent 0.0009.

2.1 Bandwidth Enhancement of the GAA by loading the rhombus shaped radiating element to the GAA short sides

In order to improve the bandwidth of the conventional GAA, a rhombus shaped radiating element is loaded into the short side of the conventional GAA as illustrated in Fig. 1. By loading the rhombus on the short sides, the capacitive reactance and the current path of the radiating elements are increased. Hence the enhancement of the GAA impedance bandwidth. To obtain the broadside radiation pattern, the proposed GAA is fed with the 50 Ω coaxial probe, located at the joint of the long and short sides center elements of the antenna. The optimized dimensions of the proposed wideband GAA are tabulated in Table 1.

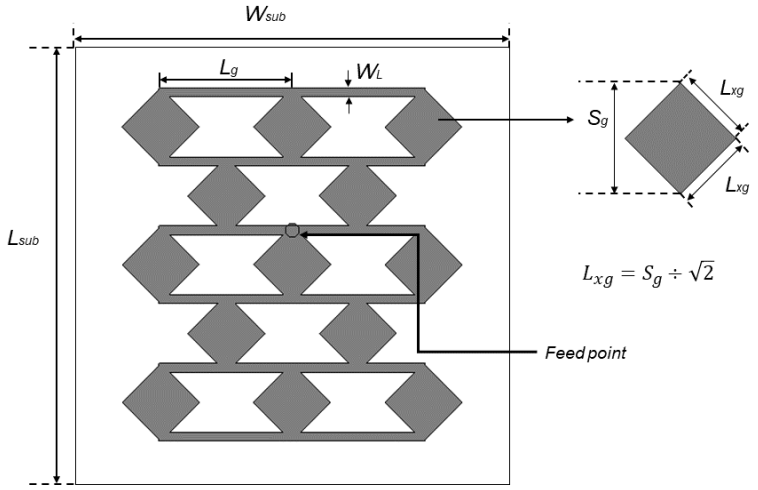

Fig. 1. Design of the proposed Wideband Rhombus Loaded Grid Array Antenna

Table 1. Optimized dimension of the proposed wideband GAA

Parameters	L_{sub}	W_{sub}	h	W_L	L_g	S_g	L_{xg}
Dimension (mm)	25	25	0.787	0.5	7.7	4.4	3.04

2.1.1 Amplitude-Tapered Wideband GAA with Variable-Sized Radiating Elements

The amplitude-tapering (AT) technique is implemented on the proposed wideband GAA for side-lobe level (SLL) reduction. The AT is performed so that the highest excitation is located at the centre area of the GAA. The amplitude is reduced toward the radiating elements at the edges of the GAA. By implementing the AT in the aforementioned manner, the radiating elements located at the centre row of the GAA are carrying the maximum currents and vice versa. The proposed AT wideband GAA is as shown in Fig. 2 and the optimized dimension are tabulated in Table 2. To provide a better understanding of the AT wideband GAA, the corresponding current distribution of the proposed wideband GAA before and after amplitude tapering is illustrated in Fig 3. As can be seen, when the AT is applied, the current flowing on the sides radiating elements is decreased which leads to the side lobes level reduction.

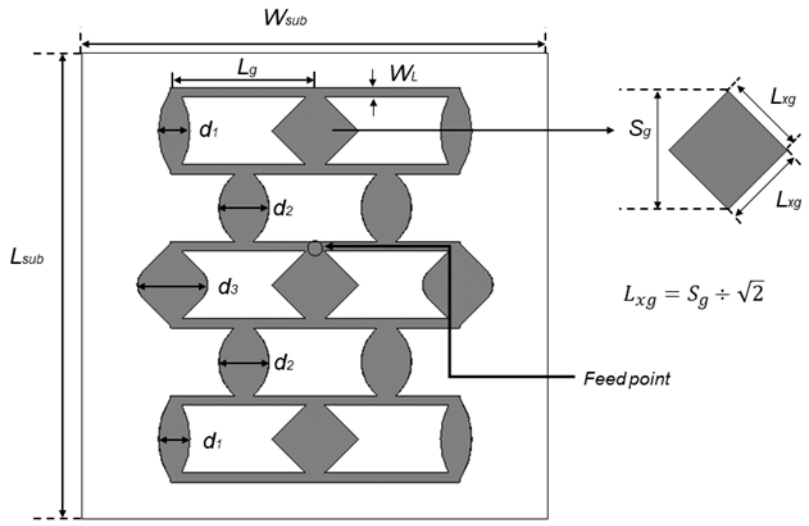

Fig.2 . Proposed Wideband Rhombus Loaded Grid Array Antenna with AT

Table 2. . Optimized dimension of the proposed wideband Rhombus Loaded GAA with AT

Parameters	L_{sub}	W_{sub}	h	L_g	S_g
Dimension (mm)	25	25	0.787	7.8	4.6
Parameters	L_{xg}	W_L	d_1	d_2	d_3
Dimension (mm)	3.11	0.5	1.7	2.7	3.77

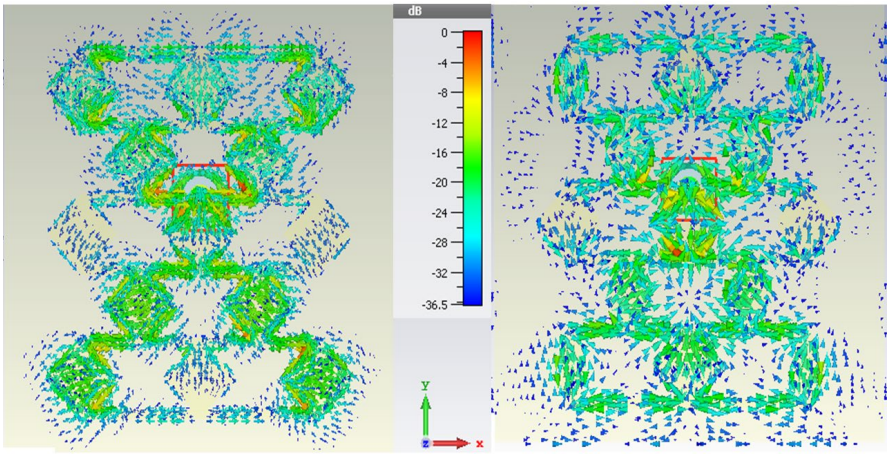

(a) (b)

Fig. 3. Current Distribution of the proposed wideband Rhombus Loaded GAA (a) Without AT and (b) With AT

2.1.2 Simulation Results of the proposed Rhombus Loaded Wideband GAA

The proposed wideband GAA is modelled using the Computer Simulation Technology (CST) software. Fig 4 shows the comparison of the obtained S11 for the considered GAAs with and without AT. It can be observed that the proposed wideband GAA provides a -10 dB impedance bandwidth of around 16:07% which is ranging from 27.5 to 32 GHz. The proposed GAA covers the entire 28 GHz frequency band for 5G recommended by the Federal Communications Commission (FCC) [17]. The simulated gain and VSWR performance for the proposed wideband GAA with and without AT is shown in Fig 5. The simulated GAAs show broadband impedance matching with VSWR < 2.0 and V SWR < 2.5 over the entire operational bandwidth for GAA without AT and with AT, respectively. As can be seen from Fig. 5, the maximum achieved gain is approximately 14.3 dBi and 14.8 dBi, without AT and with AT, respectively. Hence, the impact of the AT on the bandwidth and gain performance of the GAA is negligible.

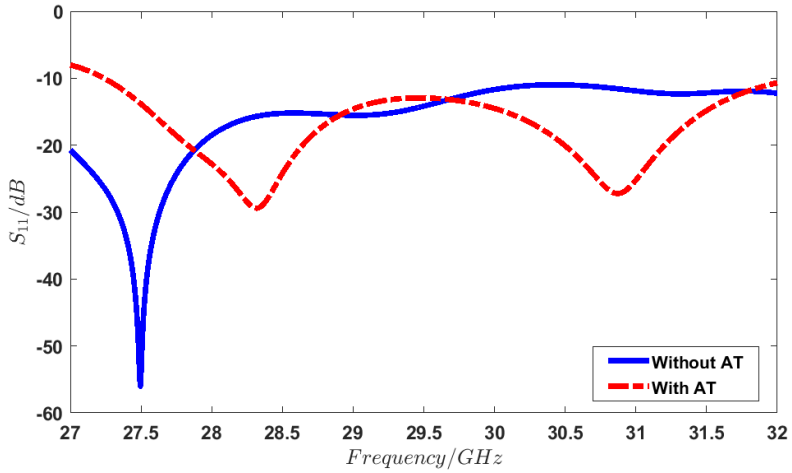

Fig. 4. Comparison of the S11 with and without AT for the Wideband Rhombus Loaded GAA

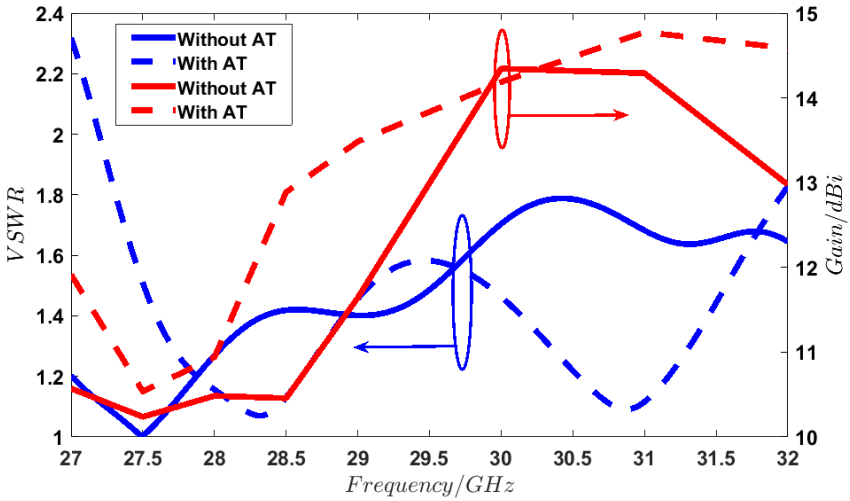

Fig. 5. Comparison of the simulated gain and VSWR performance of the proposed wideband Rhombus Loaded GAA with and without AT

Fig. 6. shows the simulated radiation pattern of the proposed antenna at 27.5 GHz on the E- and H-planes in subplots (a) and (b), respectively. Results are compared for designs with and without

the implementation of AT. Similar results are shown in Figs. 7 and 8 for the 29 GHz and 32 GHz frequencies, respectively. As can be observed from Fig. 6(a), the SLL of the wideband GAA for the E-plane co-polar pattern is around -4 dBi at 27.5 GHz and enhanced to -11 dBi with AT applied on the wideband GAA. The enhancement of the SLL of the E-plane co-polar radiation pattern for 29 GHz and 32 GHz are more significant. At 29 GHz, the SLL from originally -5 dBi and improved to -15 dBi, with the improvement of 10 dBi. As for 32 GHz, the SLL for E-plane radiation pattern is -10 dBi and -25 dBi for wideband GAA without AT applied and with AT applied, respectively. By implementing the AT on the wideband GAA, it allows the higher current distributed over the central elements and lower current distributed at the radiating elements on the side. By having these current distribution, it allows the increase in the gain of the main beam at the broadside direction and reduce the gain at the SLL.

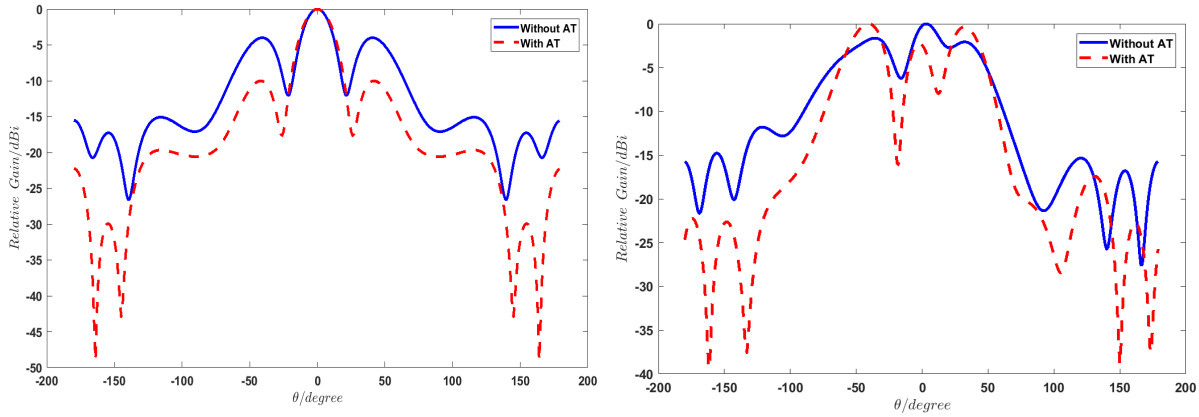

(a) (b)

Fig. 6. Comparison of the simulated co-polar radiation pattern at 27.5 GHz with and without AT for (a) E-plane and (b) H-plane for wideband rhombus loaded GAA

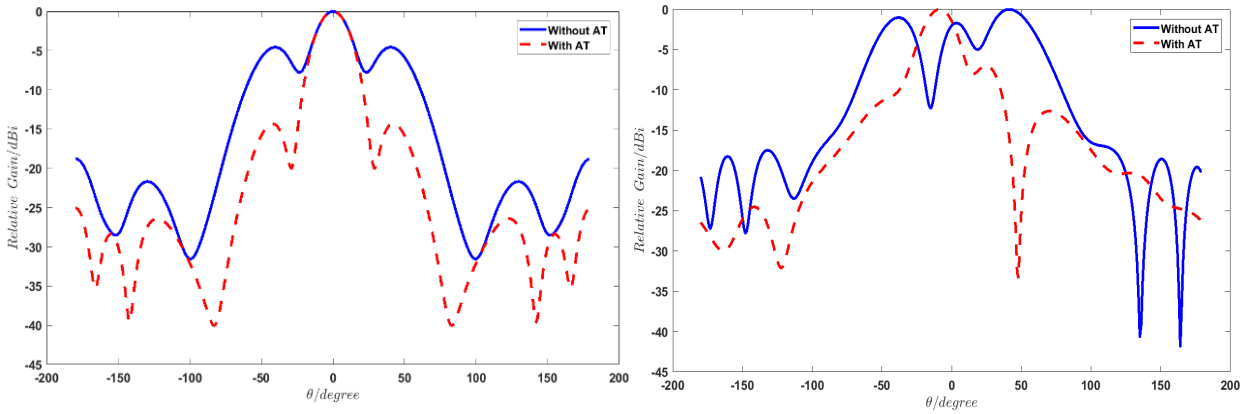

(a) (b)

Fig. 7. Comparison of the simulated co-polar radiation pattern at 29 GHz with and without AT for (a) E-plane and (b) H-plane for wideband rhombus loaded GAA

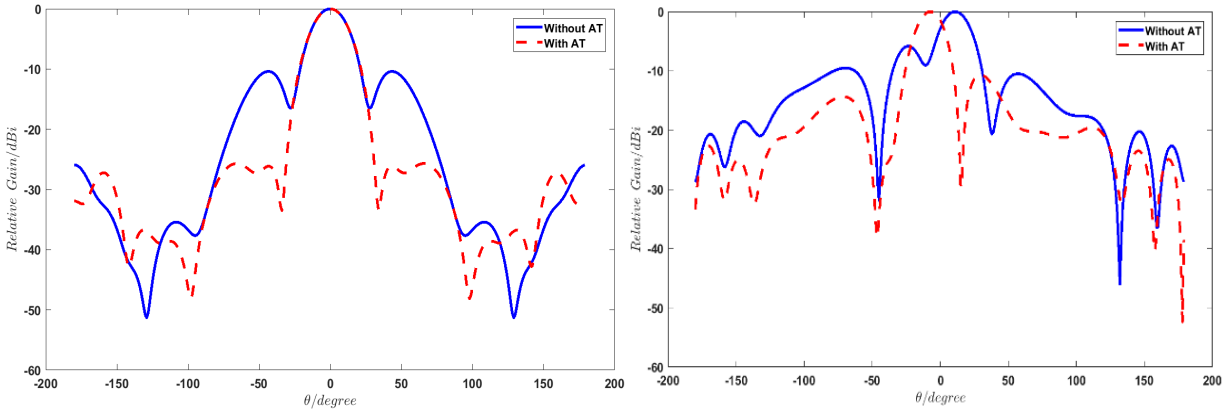

Fig. 7. Comparison of the simulated co-polar radiation pattern at 32 GHz with and without AT for (a) E-plane and (b) H-plane for wideband rhombus loaded GAA

However, it is worthwhile to note that AT did not implied a significant enhancement of the SLL for the H-plane co-polar radiation pattern at 27.5 GHz. This can be mainly attributed to the improper control over the current phase alignment over the GAA radiating elements. As it can be observed from Fig. 6(b), the H-plane radiation pattern of the original rhombus loaded wideband GAA at 27.5 GHz, the main beam direction is slightly tiled and with presence of grading lobes. As a result, the implementation of the AT is ineffective on the H-plane co-polar radiation performance at 27.5 GHz. Similar trends are observed for the at H-plane co-polar radiation pattern for 29 GHz and 32 GHz, where the AT does not give significant enhancement on the grading lobes reduction. Besides that, the insignificant effect of the AT can also be attributed to the arrangement of the grid and the AT method implementation illustrated in Fig. 2.

2.2 Bandwidth Enhancement of the GAA using staircase radiating element on the short sides of the GAA

In this section, we proposed an alternative bandwidth enhancement technique by replacing the short side radiating element of the conventional GAA with staircase radiating element as illustrated in Fig. 8. Similar to the rhombus loaded GAA, when the staircase is replaced the conventional slot, the current path is longer and the capacitive effect is improved and lead to the enhancement on bandwidth. However, due to the multiple steps in the staircase, this design provides more flexibility in the bandwidth optimization and the current path is much longer as compared to the rhombus loaded GAA. The optimized dimension of the proposed Staircase microstrip GAA is tabulated in Table 3.

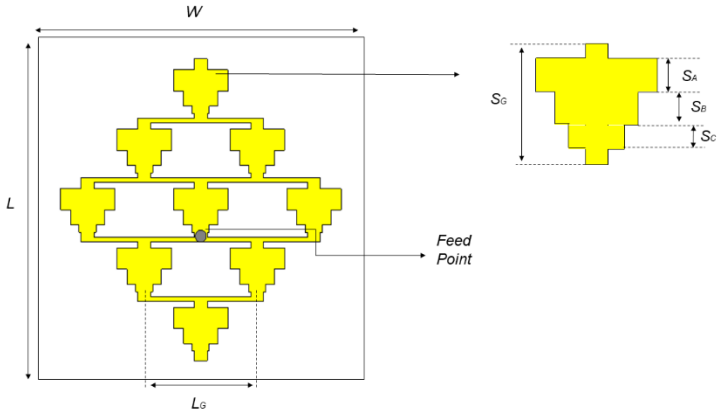

Fig. 8. Wideband Staircase GAA

Table. 3. Optimized dimension of the wideband staircase GAA

Parameters	L	W	h	L_G	S_G
Dimension (mm)	25	25	0.787	8.5	4.25
Parameters	S_A	S_B	S_C		
Dimension (mm)	1.4	1	0.5		

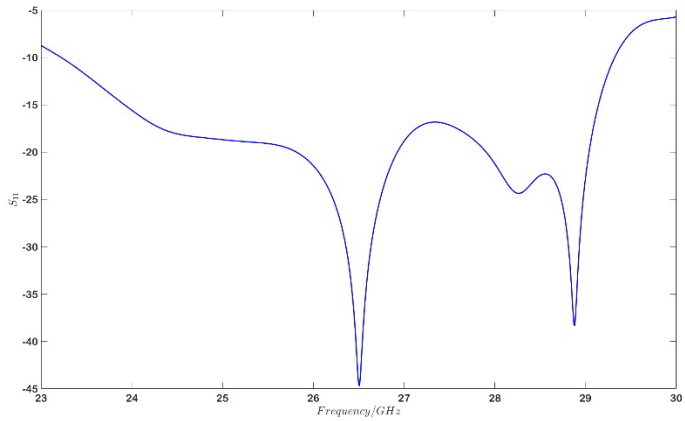

Fig.9. Simulated S11 of the Wideband Staircase Grid Array Antenna

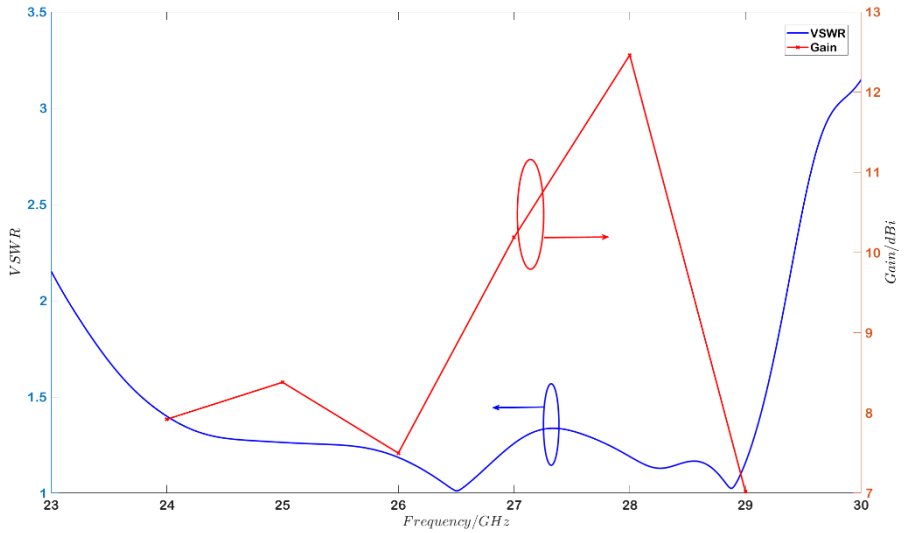

Fig. 10. Simulated gain and VSWR performance of the proposed wideband

Fig.9 show the simulated S11 of the proposed rhombus loaded GAA. The -10 dB impedance bandwidth is around 21% which is ranging from 23.5 GHz to 29.5 GHz. The VSWR of the proposed wideband staircase antenna is less than 1.5 as illustrated in Fig.10 which indicates that the proposed antenna has a good matching over the frequency band of interest. Thus, the proposed antenna cover the entire frequency band for 5G millimeter wave proposed by both the European Conference of Postal and Telecommunications Administration (CEPT) and the Federal Communications Commission (FCC). In addition, the proposed antenna show a maximum achieved gain of around 12.5 dBi. The gain slightly drops as compare to the previous wideband rhombus loaded GAA mainly due to the fact that some elements are removed from the grid to reduce the side lobes level of the proposed antenna.

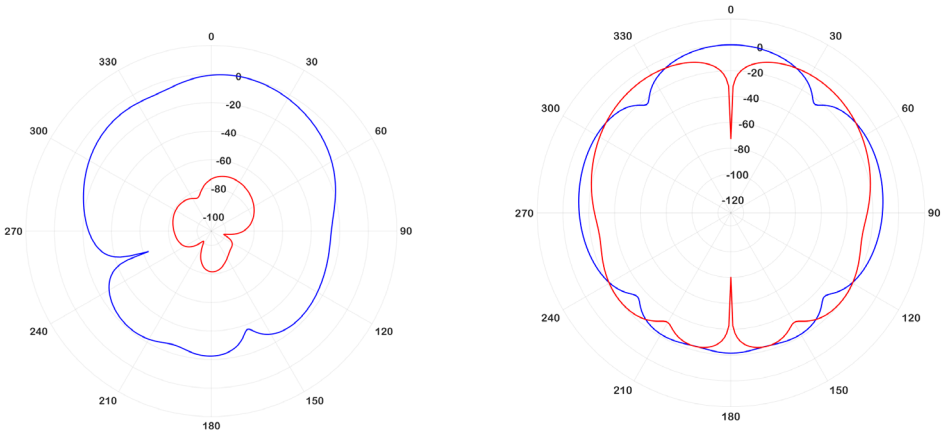

(a) (b)

Fig. 11. Simulated Co-Polar (Blue Line) and Cross-Polar (Red Line) Radiation Pattern at 24 GHz for (a) E-plane and (b) H-plane

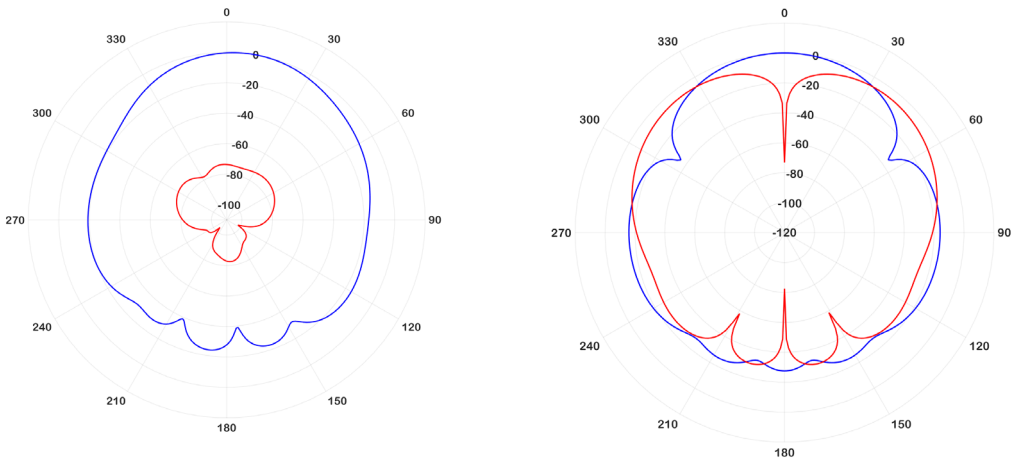

Fig. 12. Simulated Co-Polar (Blue Line) and Cross-Polar (Red Line) Radiation Pattern at 26 GHz for (a) E-plane and (b) H-plane

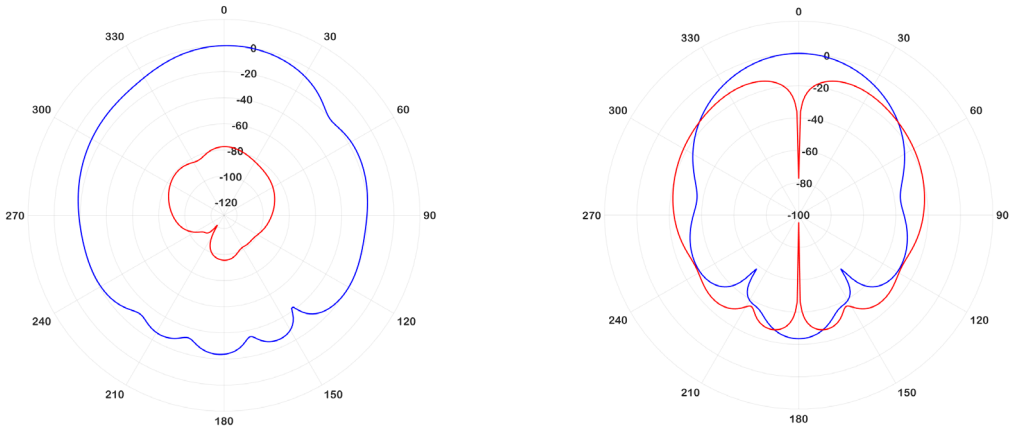

Fig. 13. Simulated Co-Polar (Blue Line) and Cross-Polar (Red Line) Radiation Pattern at 28 GHz for (a) E-plane and (b) H-plane

Fig. 11 shows the simulated radiation pattern of the proposed wideband staircase GAA at 26 GHz on the E- and H-planes in subplots (a) and (b), respectively. Similar results are shown in Figs. 12 and 13 for the 26 GHz and 28 GHz frequencies, respectively. As can be observed from Figs. 11, 12 and 13, the main beam direction in the E-plane is tilted by 10° in the clockwise direction as the feeding of the antenna is not located exactly on the center of the radiating patch. In addition, the cross polarization of the proposed antenna is very low at E-plane. However, the cross polarization of the proposed antenna over the H-plane is only low at the main beam direction but remains high over the other directions.

2.3 Discussion

Table 4 shows a comparison of the performance of recent developed planar mmWave array antennas. In [4], it has been proposed to use the LTCC technology to enhance the bandwidth performance of the conventional GAA with achievable bandwidth of around 15.6%, while in [9] a thicker substrate is proposed to get wider bandwidth of around 13% for the conventional

miniaturized GAA. In our work, we manage to achieve a wider bandwidth of 16% and 21% while keeping a low volume profile. In addition, comparing to other high gain antenna solutions which proposed FSS [3], multilayer stacking [2] and SIW feeding [1], it is clear that the GAA manage to provide a good gain performance at low profile. However, due to the feeding of the antenna must be located in the crossing between the short side and long sides of the center, the main beam is tilted as compare to other proposed solution. It is also worthwhile to note that the cross polarization of the proposed GAA at H-plane is only low over the main beam direction, but remaining high in other direction.

Table 4. Performance comparison among the existing High Gain antenna for mmWave application where *fc* is the center frequency and λo is the wavelength of the center frequency

Ref.	**Antenna's Types**	***fc* (GHz)**	**Dimension**	**Bandwidth (%)**	**Peak Gain (dB)**	**Technique**
[18]	Phased Array	28	$6.54\lambda o \times 5.93\lambda o \times 0.21\lambda o$	8.21	13.97	Multilayer substrate and using SIW Feeding
[19]	Linear Array	28	$\lambda o \times 3\lambda o \times 0.12\lambda o$	6.3	21.4	Multilayer stacking
[12]	Dielectric Patch	28	$3\lambda o \times 3\lambda o \times 0.12\lambda o$	15.54	17.78	Cascade FSS
[16]	GAA	60	$3\lambda o \times 3\lambda o \times 0.12\lambda o$	15.6	17.7	LTCC
[20]	GAA	28	$3\lambda o \times 3\lambda o \times 0.12\lambda o$	13	7.3	PCB Substrate
Rhombus Loaded GAA	GAA	28	$2.33\lambda o \times 2.33\lambda o \times 0.07\lambda o$	16.07	14.8	PCB Substrate
Staircase GAA	GAA	28	$2.8\lambda o \times 2.8\lambda o \times 0.07\lambda o$	21%	12.5	PCB Substrate

3 mmWave Antenna Array based on Gapwaves Waveguide Technology for 5G Applications

Unlicensed wide frequency bands in mmWave provide the opportunity to develop new technologies supporting the required massive data rates. Although the wide bandwidth can be an advantage in the mmWave band, there exist challenges in the implementation of primary transmission technologies. For example, metal waveguide and substrate-based PCBs suffer from manufacturing difficulties and substantial losses [21] in mmWave frequencies, respectively.

As a solution to the above, the Gapwaves waveguide technology offers a robust and low loss solution for the mmWave frequencies [22]. This technology creates a transmission line with confined fields between two PEC strips by using the electromagnetic waves rejection in PEC-PMC parallel plate waveguide with separation distance lower than a quarter wavelength. Commonly, a bed of pins is used for realizing an artificial magnetic conductor. Gapwaves waveguides allow a robust implementation of transmission lines and components without needing an electrical contact between two layers. Hence, the Gapwaves waveguide technology offers good performance at a reasonable expense.

A slot array antenna based on Gapwaves waveguide technology has been designed for 5G applications in mmWaves. The array antenna consist of 8 x 8 slots organized in 8-slot subarrays in 8 columns and a single row, which is shown in Fig. 13. The distance between the centers of two adjacent subarrays is half of the free-space wavelength at highest frequency of the bandwidth. This spacing allows antenna to scan ±45° in azimuth plane without appearance of any grate lobes. The antenna's polarization is horizontal. The subarray is a slotted waveguide with series, resonant, center-fed and identical slots.

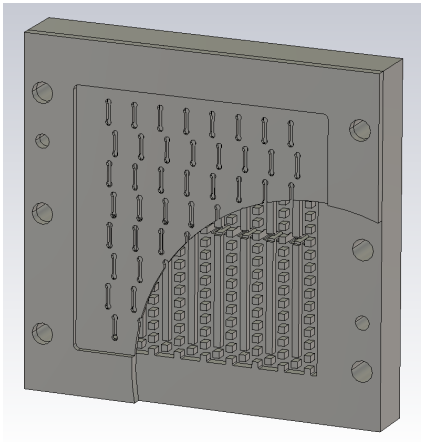

Fig. 14. View of antenna array. A part of slot layer is cut to make distribution layer visible.

The antenna covers frequency band from 26.5 to 29.5 GHz considering matchings and radiation patterns. The simulated embedded matching and isolation are better than -16 dB, while the simulated active matching is better than -10 dB at all scan angles. Fig. 15 shows the embedded matching and isolation for first four ports separately. The active matching for scan angles 0, 15, 30 and 45 degrees are depicted in Fig. 16. Due to symmetry in the structure, results for negative scan angles are not shown. The antenna provides approximately 23 dBi of gain and radiation pattern in azimuth plane at highest frequency of bandwidth is shown in Fig. 17.

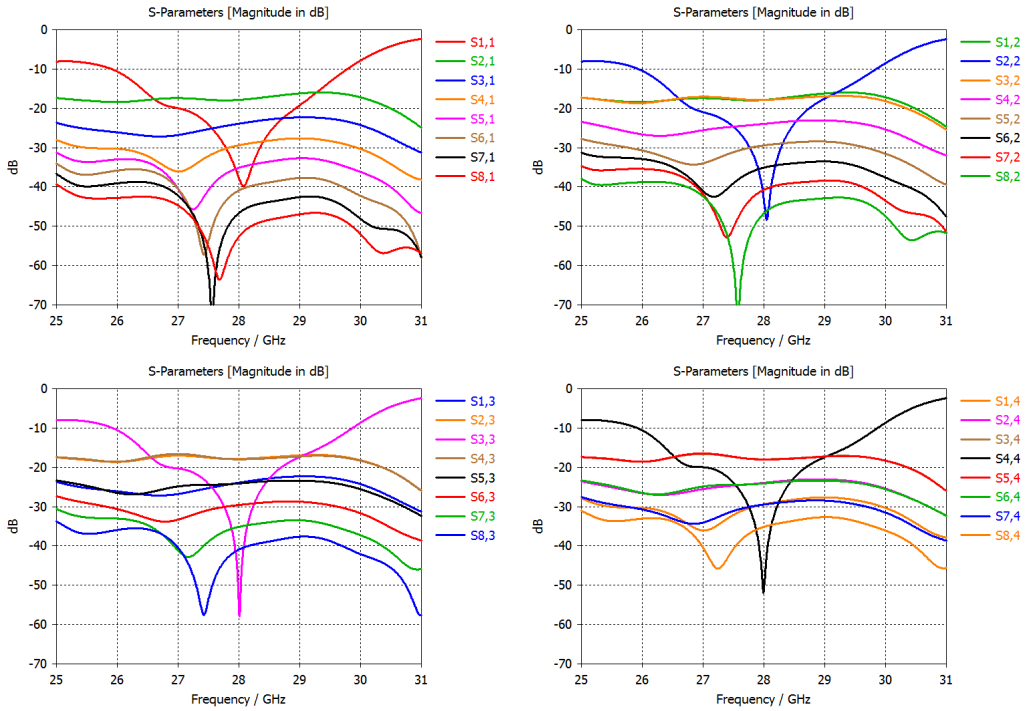

Fig. 15. Simulated embedded scattering parameters for ports 1 to 4.

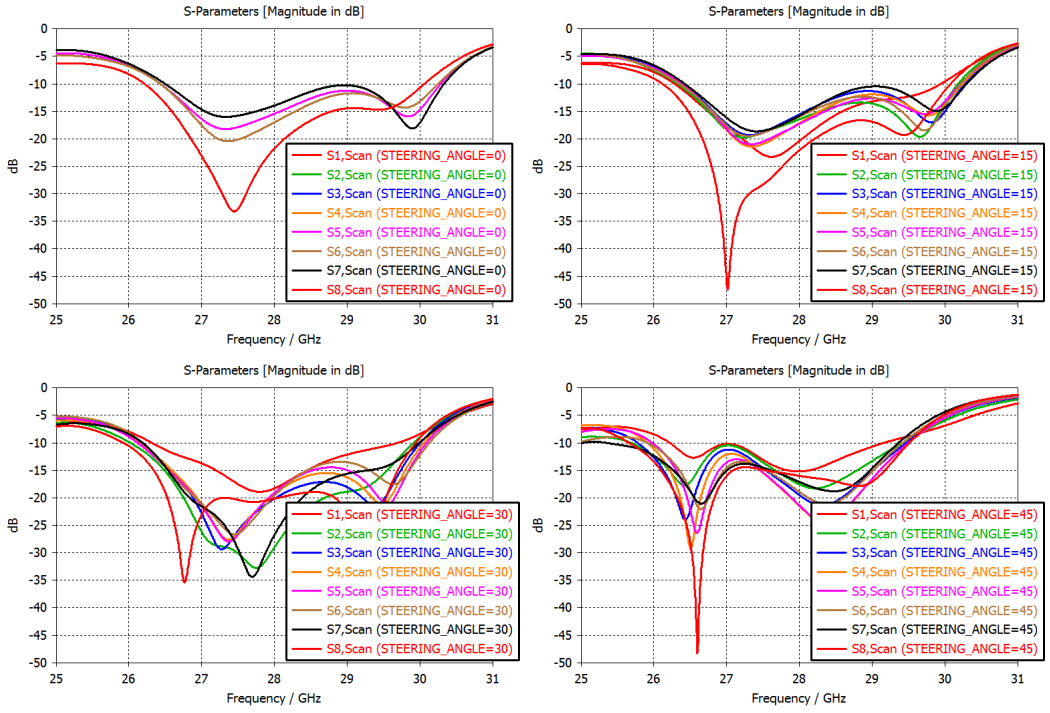

Fig. 16. Simulated active matching for scanning angles of 0, 15, 30 and 45.

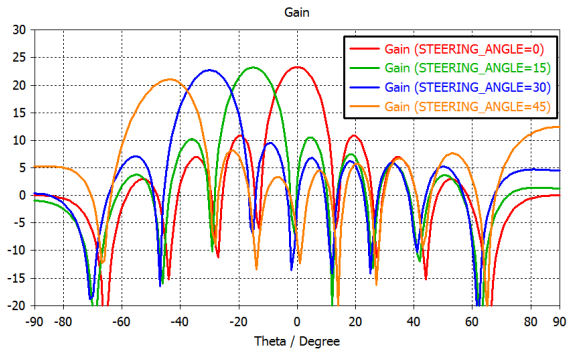

Figure 17. Simulated radiation pattern for azimuth scanning.

4 Conclusions

In this paper, we proposed two different approach in designing the high gain millimeter wave array antenna. First, we proposed to design the wideband high gain grid array antenna based on the conventional microstrip technology. There are in total of two microstrip grid array antenna geometry have been proposed to enhance the bandwidth of the conventional microstrip grid array antenna. First, we proposed to loaded the rhombus shaped on the short side of the conventional grid array antenna. The bandwidth performance of the grid array antenna is enhanced by loading the rhombus on the short radiating sides of the conventional GAA. The amplitude tapering technique has been applied to reduce the side-lobe levels of the proposed wideband GAA. The dimensions of the proposed antenna are 25 × 25 × 0.787 mm^3. The simulation results show that the proposed wideband GAA having an impedance bandwidth of 16.07% with a maximum gain of 14.8 dBi. To further enhance the bandwidth so that the proposed grid array antenna can cover both the 24 GHz Band and 28 GHz Band proposed for 5G, a staircase geometry is proposed to replace the rhombus shaped on the short sides. The dimensions of the proposed rhombus loaded grid array antenna are 28 × 28 × 0.787 mm^3. The simulation results show that the proposed wideband GAA having an impedance bandwidth of 21% with a maximum gain of 12.5dBi. As it can be observed, although these PCB grid array antenna manage to provide a very wide bandwidth, but the gain performance is remain around 13 dBi which is still remain insufficient for the 5G mmWave base station. Therefore, in the second approach, we proposed to use the recently introduced Gap waveguides technology. The proposed gap waveguide antenna covers frequency band from 26.5 to 29.5 GHz considering matchings and radiation patterns. The proposed antenna provide scanning capabilities up to ±45° in azimuth plane without appearance of any grate lobes. The antenna provides approximately 23 dBi of gain over the frequency band of interest. In our future works, we will focus on the design of the millimeter wave antenna based on the gap waveguide technology. We will first enhance the bandwidth performance of our proposed antenna so that it could cover the 24 and 28 GHz millimeter wave band proposed for 5G. We will also further enhance the antenna performance such as gain and scanning capabilities performance. We will also investigate the possibility in design these proposed antenna with dual linear polarization, circular polarization or dual circular polarization which wider the application of these mmWave antenna.

Appendix A. List of Publications

1. Wai Yan Yong and Andrés Alayón Glazunov, “High Gain, Wideband Grid Array Antenna for 28 GHz 5G Base Station,” *European Conference on Antenna and Propagation (EuCAP)* 2019, (Presented), Krakow, Poland.
2. Alireza Bagheri, Carlo Bencivenni, Andrés Alayón Glazunov, “mmWave Antenna Array based on Gapwaves Waveguide Technology for 5G Applications,” *International Conference on Electromagnetics in Advanced Applications (ICEAA) 2019*, (Accepted), Granada, Spain.

References

[1] T. S. Rappaport, Y. Xing, J. MacCartney, A. F. Molisch, E. Mellios, and J. Zhang, "Overview of Millimeter Wave Communications for Fifth-Generation (5G) Wireless Networks-with a focus on Propagation Models," *IEEE Trans. Antennas Propag.*, vol. 65, no. 12, pp. 6213–6230, 2017.

[2] J. Zhang, X. Ge, Q. Li, M. Guizani, and Y. Zhang, "5G M illimeter -Wave Antenna Array : Design and Challenges," *IEEE Wirel. Commun.*, vol. 24, no. April, pp. 106–112, 2017.

[3] B. and Ai *et al.*, "On Indoor Millimeter Wave Massive MIMO Channels: Measurement and Simulation," *IEEE J. Sel. Areas Commun.*, vol. 35, no. 7, pp. 1678–1690, 2017.

[4] A. B. and Sherif, M. S. H. and Kazi, M. and Shahid, D. and Linglong, and R. Jonathan, "Millimeter-Wave Massive MIMO Communication for Future Wireless Systems: A Survey," *IEEE Commun. Surv. Tutorials*, vol. 20, no. 2, pp. 836–869, 2018.

[5] M. A. Al-Tarifi, M. S. Sharawi, and A. Shamim, "Massive MIMO antenna system for 5G base stations with directive ports and switched beamsteering capabilities," *IET Microwaves, Antennas Propag.*, vol. 12, no. 10, pp. 1709–1718, 2018.

[6] R. Baxter, N. Hastings, A. Law, and E. J. . Glass, "Design of Energy and Cost-Efficient Massive MIMO Arrays," *Proc. IEEE*, vol. 104, no. 3, pp. 586–606, 2016.

[7] M. H. Dahri, M. I. Abbasi, M. H. Jamaluddin, and M. R. Kamarudin, "A Review of High Gain and High Efficiency Reflectarrays for 5G Communications," *IEEE Access*, vol. 6, pp. 5973–5985, 2018.

[8] Y. Hu, W. Hong, and Z. H. Jiang, "A Multibeam Folded Reflectarray Antenna with Wide Coverage and Integrated Primary Sources for Millimeter-Wave Massive MIMO Applications," *IEEE Trans. Antennas Propag.*, vol. PP, no. c, pp. 1–1, 2018.

[9] Y. Miura, S. Member, J. Hirokawa, S. Member, and M. Ando, "Double-Layer Full-Corporate-Feed Hollow- Waveguide Slot Array Antenna in the 60-GHz Band," *IEEE Trans. Antennas Propag.*, vol. 59, no. 8, pp. 2844–2851, 2011.

[10] T. Tomura, S. Member, Y. Miura, S. Member, and M. Zhang, "A 45 Linearly Polarized Hollow-Waveguide Corporate-Feed Slot Array Antenna in the 60-GHz Band," *IEEE Trans. Antennas Propag.*, vol. 60, no. 8, pp. 3640–3646, 2012.

[11] K. Wu, Y. J. Cheng, T. Djerafi, and W. Hong, "Substrate-integrated millimeter-wave and terahertz antenna technology," *Proc. IEEE*, vol. 100, no. 7, pp. 2219–2232, 2012.

[12] M. Asaadi, I. Afifi, and A. R. Sebak, "High Gain and Wideband High Dense Dielectric Patch Antenna Using FSS Superstrate for Millimeter-Wave Applications," *IEEE Access*, vol. 6, pp. 38243–38250, 2018.

[13] Z. Chen, Y. P. Zhang, A. Bisognin, D. Titz, F. Ferrero, and C. Luxey, "An LTCC Microstrip Grid Array Antenna for 94-GHz Applications," *IEEE Antennas Wirel. Propag. Lett.*, vol. 14, pp. 1279–1281, 2015.

[14] T. Zhang, L. Li, H. Xia, X. Ma, and T. J. C. Cui, "A low-cost and high-gain 60-GHz differential phased array antenna in PCB process," *IEEE Trans. Components, Packag. Manuf. Technol.*, vol. 8, no. 7, pp. 1281–1291, 2018.

[15] B. Zhang and Y. P. Zhang, "Analysis and Synthesis of Millimeter-Wave Microstrip Grid-Array Antennas," *IEEE Antennas Propag. Mag.*, vol. 6, no. 53, pp. 42–55, 2011.

[16] B. Zhang and Y. P. Zhang, “Grid array antennas with subarrays and multiple feeds for 60-GHz radios,” *IEEE Trans. Antennas Propag.*, vol. 60, no. 5, pp. 2270–2275, 2012.

[17] “The FCC 5G Fast Plan,” *FCC*, 2018. [Online]. Available: https://www.fcc.gov/5G.

[18] S. Park, D. Shin, S. Park, S. Member, and A. Abstract, “Low Side-Lobe Substrate-Integrated-Waveguide Antenna Array Using Broadband Unequal Feeding Network for Millimeter-Wave Handset Device,” *IEEE Trans. Antennas Propag.*, vol. 64, no. 3, pp. 923–932, 2016.

[19] P. A. Dzagbletey and Y. Jung, “Stacked Microstrip Linear Array for Millimeter-Wave 5G Baseband Communication,” *IEEE Antennas Wirel. Propag. Lett.*, vol. 17, no. 5, pp. 780–783, 2018.

[20] M. S. and Yahya and S. K. A. Rahim, “15GHz Grid Array Antenna for 5G Mobile Communications System,” *Microw. Opt. Technol. Lett.*, vol. 58, no. 12, pp. 2977–2980, 2016.

[21] C. Bencivenni, T. Emanuelsson, and M. Gustafsson, “Gapwaves Platform Integrates 5G mmWave Arrays,” *Microwave Journal 62*, p. 62(2), 2019.

[22] P. Kildal, E. Alfonso, S. Member, E. Rajo-iglesias, and S. Member, “Local Metamaterial-Based Waveguides in Gaps Between Parallel Metal Plates,” *IEEE Antennas Wirel. Propag. Lett.*, vol. 8, pp. 84–87, 2009.